ELSEVIER

Biomolecular Engineering
17 (2000) 23–36

Biomolecular Engineering

www.elsevier.com/locate/geneanabioeng

Review

# Micromachined interfaces: new approaches in cell immunoisolation and biomolecular separation

Tejal A. Desai [a,*], Derek J. Hansford [b], Mauro Ferrari [b]

[a] *Department of Bioengineering (MC 063), College of Engineering, University of Illinois at Chicago, 851 South Morgan Sreet, Chicago IL 60607-7052, USA*

[b] *Biomedical Engineering Center, The Ohio State University, Columbus OH 43210, USA*

Received 25 May 2000; received in revised form 24 July 2000; accepted 24 July 2000

**Abstract**

As a novel therapeutic application of microfabrication technology, a micromachined membrane-based biocapsule is described for the transplantation of protein-secreting cells without the need for immunosuppression. This new approach to cell encapsulation is based on microfabrication technology whereby immunoisolation membranes are bulk and surface micromachined to present uniform and well-controlled pore sizes as small as 10 nm, tailored surface chemistries, and precise microarchitecture. Through its ability to achieve highly controlled microarchitectures on size scales relevant to living systems (from μm to nm), microfabrication technology offers unique opportunities to more precisely engineer biocapsules that allow free exchange of the nutrients, waste products, and secreted therapeutic proteins between the host (patient) and implanted cells, but exclude lymphocytes and antibodies that may attack foreign cells. Microfabricated inorganic encapsulation devices may provide biocompatibility, in vivo chemical and mechanical stability, tailored pore geometries, and superior immunoisolation for encapsulated cells over conventional encapsulation approaches. By using microfabrication techniques, structures can be fabricated with spatial features from the sub-micron range up to several millimeters. These multi-scale structures correspond well with hierarchical biological structures, from proteins and sub-cellular organelles to the tissue and organ levels. © 2000 Published by Elsevier Science B.V.

*Keywords:* Microfabrication; Biocapsule; Biomolecular separation

## 1. Cellular immunoisolation

The immunoisolation of transplanted cells and tissue emerged as an extremely promising method of treating hormone deficiencies arising from such diseases as Type I diabetes, Alzheimer's, and hemophilia [1–3]. Immunoisolation, in this case, refers to the physical protection or separation of cells from immunological attack. It has been demonstrated that cellular transplants, such as isolated pancreatic islets of Langerhans or hepatocytes, respond physiologically both in vitro and in vivo by secreting bioactive substances in response to appropriate stimuli, given appropriate immunoprotection. However, with the exception of autologous cells and tissue, overcoming immunologic rejection of the transplanted cells is still the greatest obstacle.

Ideally, in diabetic patients, transplantation of pancreatic islet cells (allografts or xenografts) could restore normoglycemia. However, as with most tissue or cellular transplants, the islet grafts, particularly xenografts, are subjected to immunorejection in the absence of chronic immunosuppression. To overcome this need for

*Abbreviations:* MEMS, micro electro mechanical systems; BioMEMS, microfabricated devices for biomedical applications; CNS, central nervous system; C1q, complement molecule; IgM, immunoglobulin M; IgG, immunoglobulin G; MAC, membrane attack complex; HF, hydrofluoric acid; EDP, ethylene diamine pyrocatechol; PSG, phosphosilicate glass; Poly or polysilicon, polycrystalline silicon; LSN, low stress nitride; LPCVD, low pressure chemical vapor deposition; CMP, chemical mechanical polishing; KOH, potassium hydroxide; SEM, scanning electron micrograph; PMMA, poly methyl methacrylate; PPMA, poly propyl methacrylate; PEMBA, poly ethyl butyl methacrylate; kD, kilo daltons; MW, molecular weight; SI, stimulatory index.

* Tel.: +1-312-413-8723; fax: +1-312-996-5921.
*E-mail address:* tdesai@uic.edu (T.A. Desai).

1389-0344/00/$ - see front matter © 2000 Published by Elsevier Science B.V.
PII: S1389-0344(00)00063-0

immunosuppressive drugs, the concept of isolating the islets from the recipient's immune system within biocompatible size-based semipermeable capsules was developed [4–6, 7]. In principle, such capsules can allow for the free diffusion of glucose, insulin, and other essential nutrients for the islets, while inhibiting the passage of larger entities such as antibodies and complement components [8]. This selective permeability can allow for the physiological functioning of the islets, while preventing acute and chronic immunorejection. Fig. 1 shows the basic structure of a polymeric microcapsule, as well as several membrane morphologies that can be obtained through different processing routes [9]. It demonstrates the thickness of the membranes used, which can greatly impede diffusion of the nutrients and insulin.

The requirements for an immunoisolating biocapsule are numerous. In addition to well-controlled pore size, the capsule must exhibit thermomechanical stability, non-biodegradability, and biocompatibility. All encapsulation methods to date have used polymeric semipermeable membranes [10–18]. However, a number of challenges remain with these current microcapsule processing techniques using polymeric materials. These membranes have exhibited insufficient resistance to organic solvents and inadequate mechanical strength — all of which eventually lead to destruction of cell xenografts [19–21]. The most common method of immunoisolation, that of polymeric microcapsules, have the disadvantage of limited retrievability and possible mechanical failure of the spherical membrane. More importantly, due to their polymeric nature, they often exhibit broad pore size distributions that allow unwanted immune components to diffuse through the membrane (Fig. 2). These characteristics may limit the use of microcapsules for non-immunosuppressed xenotransplantation [2,22].

Despite significant progress in cell transplant therapy over the last 30 years, long-term and complete immunoisolation of xenogeneic cell grafts, specifically pancreatic islets of Langerhans, via membrane encapsulation remains a much sought after therapeutic goal. Previous studies have hypothesized that pore sizes smaller than 100 nm would be effective providing immunoisolation, but more recently it has been demonstrated that these membranes still do not completely block immune molecules from reaching xenogeneic cells [2,5,23]. These problems are usually associated with membrane integrity, selectivity, and configuation. Currently, no consensus has been reached as to the ideal pore size, geometry, and surface conditions needed for complete immunoisolation of encapsulated xenogeneic cells. Although approaches involving polymeric microcapsules have yielded promising results for allogeneic cell transplantation without immunosuppression [7], few approaches have been effective for xenogeneic cell

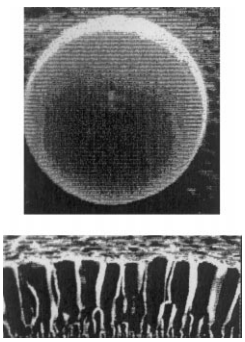

Fig. 1. Polymeric immunoisolation biocapsule and various membrane structures [9].

encapsulation. The shortage of allogeneic human donors makes xenograft immunoisolation an extremely sought after goal in cell transplant therapy. Moreover, the clinical success of encapsulated islet transplantation is still only minimal, with less than 30 documented cases of insulin independence occurring from over 250 attempts at clinical islet allo-transplantation since 1983 [24,25].

In light of these issues, a new approach to cellular immunoisolation has been developed. The microfabricated biocapsule is achieved by applying fabrication techniques originally developed for micro electro mechanical systems (MEMS), and represents one of first therapeutic applications of this technology in biomedicine. Although research on microfabricated devices for biomedical applications (BioMEMS) has rapidly expanded, it has mainly focused on the development of diagnostic tools such as electrophoretic, chromatographic, biosensor, and cell manipulation systems [26–28]. Relatively few researchers have concentrated on therapeutic applications of microfabrication technology such as neural regeneration, CNS stimulation, and microsurgery [29–31]. With this in mind, microma-

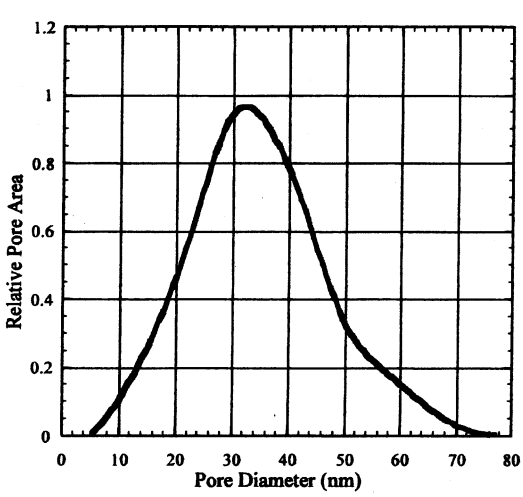


Fig. 2. Typical broad pore size distribution exhibited in polymeric membranes.

chined ultrafiltration membranes have been used to create an immunoisolation biocapsules that we can use to analyze therapeutic effectiveness and begin fundamental investigations on the physical parameters necessary for the complete immunoisolation of cells. Selecting an appropriate cut-off dimension for the immunoisolation membrane is just one of the many design parameters to be considered. Permeability of glucose, insulin, and other metabolically active products, must be high enough to insure islet functionality and therapeutic effectiveness. Additionally, pore size-based separation of immune molecules may not be sufficient to prevent immunorejection — other physical parameters such as diffusion length, surface topography, and surface chemistry must also be investigated.

Utilizing bulk and surface micromachining and microfabrication, membrane-based biocapsules can be engineered to have uniform and well-controlled pore sizes, channel lengths, and surface properties. This precise control offers the unique ability to selectively vary parameters in order to monitor the passage of a variety of stimuli and immunomolecules to target cells. By virtue of their biochemical inertness and relative mechanical strength, silicon and its oxides and nitrides offer an alternative to the more conventional organic biocapsules. These capsules can provide the advantages of mechanical stability, uniform pore size distribution, and chemical inertness. By taking advantage of silicon bulk and surface material properties, structures can be engineered to perform specific functions. Microfabrication technology may be advantageous in the field of tissue engineering by creating precisely controlled microenvironments to stimulate and enhance transplanted cell behavior. Micromachined capsules may provide advantages over conventional encapsulation approaches due to their mechanical stability, uniform pore size distribution, chemical inertness, geometry, and retrievability.

A further, and perhaps more important, advantage of microfabrication technology is the ability to fabricate membranes of specific pore size, allowing one to optimize the biocapsules specifically for the encapsulation of pancreatic islets or any given cell type. Current polymeric biocapsules have not been able to achieve uniform pore size membranes in the 10s of nm range. By contrast, we have developed several variants of microfabricated diffusion barriers, containing pores with uniform dimensions as small as 20 nm [32]. Furthermore, improved dynamic response of islets tissue can be obtained due to the reduced membrane thickness (9 μm) of microfabricated membranes compared to polymeric membranes (100–200 μm). It is important to retain rapid intrinsic secretion kinetics, in particular first phase insulin release [5], so as to provide physiological feedback control of blood glucose concentrations.

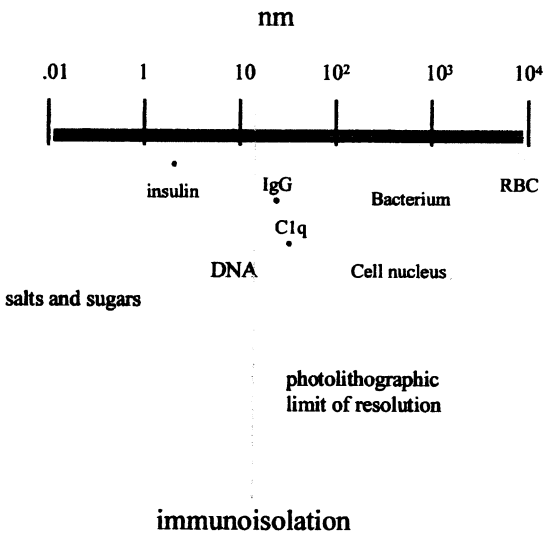


Fig. 3. Size scale of biologically relevant molecules in immunoisolation [37].

Microfabricated biocapsules with membrane pores in the 10s of nm range seem suitable for application in xenotransplantation (Fig. 3). The typical dimension of insulin, glucose, oxygen and carbon dioxide, molecules that should pass freely through the membrane, is less than 35 Å. The blockage of immune molecules, however, is a much more complicated task. Although it is relatively easy to prevent the passage of cytotoxic cells, macrophages, and other cellular immune molecules through the biocapsule, a potentially more serious problem is blockage of humoral immune components such as antibodies and cytokines as well as cell-secreted antigens. Antibody binding to a cellular transplant, by itself, usually does not cause a cytotoxic reaction. Moreover, it is the binding of the complement components that initiate the cytotoxic events [24]. Binding of C1q to IgM or two molecules of IgG can lead to the formation of a membrane attach complex (MAC) which will ultimately lyse the transplanted cell. Therefore, the immunoisolation membrane should prevent the passage of either host C1q or IgM to remain effective. Studies indicate that both C1q and IgG are completely retained by a membrane with maximum pore diameters of 30 to 50 nm [7].

All previous immunoisolation membranes, due to their polymeric nature, have found that meeting these cut-off requirements is quite difficult, due to the broad pore size distribution of real membranes. Even if only 1% of pores are larger than the cut-off goal, the pores would allow the passage of antibodies in sufficient amounts to initiate immunorejection pathways [24]. The technology involved in our microfabricated biocapsules is based on the creation of membranes with absolute and uniform pore sizes in order to better immunoisolate cellular transplants. Moreover, the po-

tential to integrate other 'smart' capabilities such as multicompartmental structure; local release of immunosuppressive drugs; biosensor incorporation, self-cleaning capabilities; modulation of angiogenesis via surface architecture or immobilized growth factors; tailoring inside and outside surfaces of capsules to elicit appropriate response, is extremely attractive. Having such capabilities on one platform may be beneficial in the long term.

## 2. Microfabricated membranes

Several research groups have used microfabrication to directly pattern a filtration membrane on a membrane for microfiltration. While this allows a simple fabrication process, it also greatly limits the minimum features that can be used for filtration. State of the art photolithography is still limited to 250 nm features, so pores smaller than this cannot be produced using standard photolithography. In fact, most university and government research microfabrication facilities are limited to much larger feature sizes for entire wafer processes. Yang et al., therefore have identified that air filtration focuses on the 1–10 μm size range, which is easily achievable through standard microfabrication. Their study investigated the use of microfabricated membranes (made of silicon nitride and parylene) for studying the effects of pore size and shape on the passage of gases [33].

Another approach to reducing the pore size using microfabrication is the use of interference lithography to produce microfiltration membranes. By using a columnated laser source and a reflecting mirror at an angle to the substrate, they produced an interference pattern on the photoresist-coated wafer. By under-exposing the pattern, rotating the wafer 90° and underexposing the wafer again, a two-dimensional pattern of 260 nm holes was produced with a spacing of 510 nm. The minimum hole size that can be fabricated using this system ($Ar^+$ laser focussed through a pinhole 1.7 m from the wafer) was 175 nm, still above the pore sizes needed for direct interaction with biomolecules [34].

Other research groups have recognized the potential of creative microfabrication for defining pores in membrane structures. A previous group at Chalmers University of Technology (Göteberg, Sweden) used a sacrificial oxide to define a flow channel between two silicon membranes. The fabrication process gave a self-aligned filter based on the etch-stop created by heavily boron-doping an opened silicon substrate. While this process has many of the advantages of a simple fabrication scheme and control over pore sizes, it had problems of doping control, pore density considerations, and a tortuous flow path [35].

Work by our multi-institutional group has focused on the use of microfabricated devices with nanopores for size-based separation of biomolecules. While the overall design has gone through several generations (see below), the basic structure and fabrication protocol for the nanopores has remained the same. By using a thermally grown silicon oxide sandwiched between two structural layers of silicon (either single crystal or polycrystalline (polysilicon)), nanopores can be fabricated in silicon structures by selectively etching the sacrificial silicon oxide in a highly selective etchant (HF) [36]. These designs give membrane structures with highly defined pore sizes.

### 2.1. Micromachined nanoporous membranes

The geometry of the pore through which the molecules are diffusing is often the main consideration for design for applications that use diffusion as the driving mechanism for separating molecules. In fact, for applications where nutrients and time-sensitive compounds are diffusing across a membrane, it is highly desirable to be able to control the diffusion length precisely. For these applications, membrane structures are more desirable than bulky filter structures. In these devices, the ability to withstand high pressures is replaced by the ability to allow fast diffusion of small molecules. The fabrication processes and flow patterns of several membrane filter designs are given below.

#### 2.1.1. The first membranes — lateral diffusion between polysilicon layers

The first design of nanoporous membranes consisted of a bilayer of polysilicon with L-shaped pore paths. An outline of the protocol use to produce these membranes is given in Fig. 4 (from [37]). As shown, the protocol used two layers of polycrystalline silicon (polysilicon or poly), with an intermediate oxide growth step. Both of the polysilicon layers were heavily boron doped to protect them during the final ethylene diamine pyrocatechol (EDP) etch through the silicon wafer. The pores were defined, as they are in all the designs, using a thin sacrificial oxide that is grown by thermal oxidation of the bottom structural layer. Anchor points were defined in the oxide layer to connect the two polysilicon layers, thus maintaining the oxide spacer distance after the oxide is removed from the final structure.

The second polysilicon layer was deposited on top of the oxide, heavily boron doped, and the entrance holes to the pores were etched through this layer. The wafer was coated with a protective phosphosilicate glass layer (PSG) for the through-wafer etch. Etch windows were defined in the backside PSG and the wafers were placed in an EDP etching bath. Once the EDP had etched

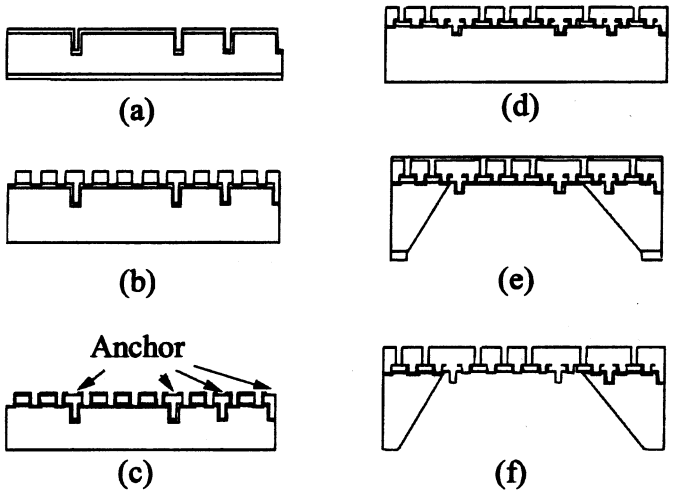


Fig. 4. Fabrication of M1 design filters: (a) etch support ridge into wafer and grow oxide; (b) deposit polysiliccon and etch exit holes; (c) grow thin sacrificial oxide to define pore widths and etch anchor points; (d) deposit second polysilicon layer and etch entrance holes; (e) pattern etch windows in protective phosphosilicate glass (PSG) and etch through silicon wafer up to protected membrane; (f) remove sacrifical and protective oxides in HF [37].

through the wafers (and stopped at the etch stop layer), the oxides (PSG and pore oxides) were removed by putting the wafers in concentrated HF. To make the pores hydrophilic, they were then cleaned in a Piranha bath ($H_2SO_4$:$H_2O_2$), which hydroxylated the silicon surface to make it hydrophilic.

The flow path of fluids and particles through the membrane is shown in Fig. 5 (adapted from [37]). As shown, fluids enter the pores through openings in the top polysilicon layer, travel laterally through the pores, make a 90° turn, and exit the pores through the bottom of the pore (where both the top and bottom polysilicon layers lay on the etch stop layer). While this design performed well for preventing the diffusion of the larger, unwanted immune system molecules, its L-shaped path slowed down and in some cases prevented the diffusion of the smaller molecules of interest. The pores in this design were fairly long, which led to the slow diffusion of the desired molecules. Also, because of the large area per pore, it was difficult to increase the pore density and thus the diffusion rate.

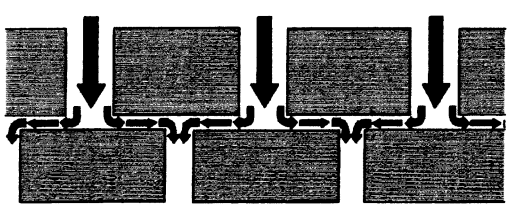

Fig. 5. Flow path through M1 filters, with lateral diffusion through the nanopores defined by sacrificial oxide ([38]).

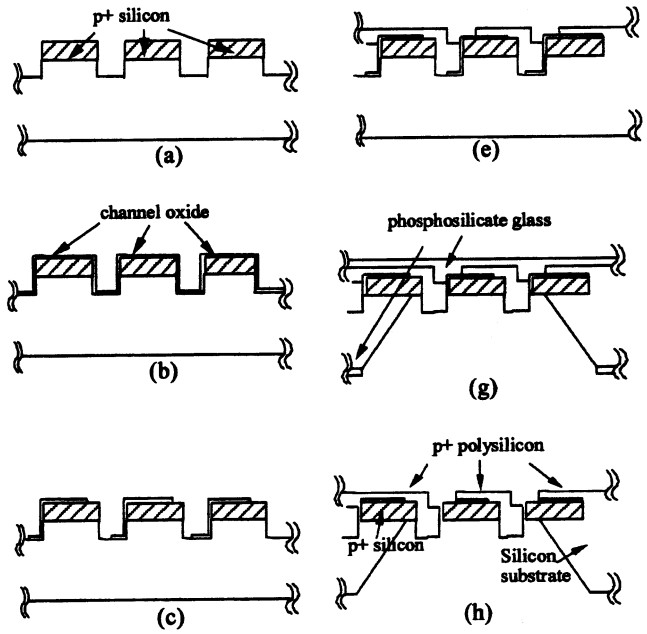


Fig. 6. Fabrication of M2C filter: (a) dope silicon with boron and etch through doped layer to define exit holes; (b) grow thin sacrificial oxide to define pore thickness; (c) etch anchor points through sacrificial oxide; (d) deposit polysilicon, dope with boron and etch entrance holes through polysilicon; (e) deposit protective PSG layer, define etch windows in backside, and etch through wafer; (f) remove protective and sacrificial oxides in HF [37].

### *2.1.2. Single crystal and straight pores*

The next design had an improvement in the production of short, straight, vertical pores through a single crystal base layer. A schematic process diagram of the design fabrication is given in Fig. 6 (from [37]). As shown in the diagram, the base layer in the structure is a heavily boron doped single crystal silicon layer. During the final etch of the wafer in EDP, this layer acts as an etch stop with a selectivity of greater than 1000:1 to the undoped silicon. To define the backside holes in the membrane structure, holes were etched through the silicon deeper than the calculated doped layer. The thin sacrificial oxide layer to define the pore size was grown on the doped silicon and the anchor points to the polysilicon layer were defined in the oxide by shifting the same mask by 1 μm from the hole pattern. Thus, the anchors were located at each pore hole, connecting the two layers for around half the pore area. A polysilicon layer was deposited over the oxide, filling in the holes and mechanically connected to the silicon base through the anchor points. The polysilicon layer was heavily boron doped and the entrance hole to the pores were defined by shifting the same mask for the holes by 1 μm in the opposite direction from the anchor points. The entire structure was then protected with PSG, the etch windows were defined on the backside, and the wafer was etched in EDP to expose the membrane. The oxides were removed in HF and the pores were made hydrophilic in a Piranha bath.

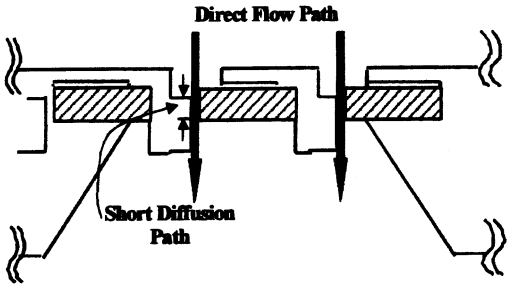


Fig. 7. Cross-section of M2 design showing direxct flow path.

This design had the advantage of direct flow paths, as shown in Fig. 7. This direct path allows the smaller molecules of interest to diffuse much quicker through the membrane, while still size-separating the larger molecules. This design also incorporated a shorter diffusion path length, based on the thicknesses of the two structural layers.

### *2.1.3. Low stress, straight pores, and precise geometrical control*

To further improve the reliability of the nanoporous membranes, several basic changes were made in the fabrication protocol from the M3 membrane design to eliminate problems with the previous diffused etch stop layer ([38]). The design of a new membrane fabrication protocol incorporated several desired improvements: a well-defined etch stop layer, precise control of pore dimensions, and a lower stress state in the membrane. The new protocol also increases the exposed pore area of the membranes. Fig. 8 shows a schematic representation of the fabrication protocol (from [38,39]), called the D1 design.

The major changes from previous protocols were the use of a buried nitride etch stop layer and the pla-

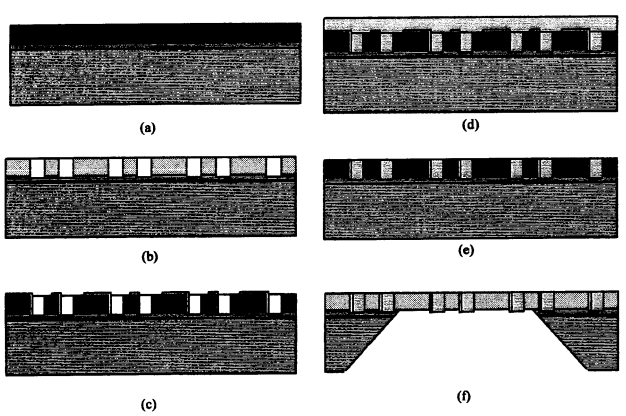


Fig. 8. D1 design process: (a) growth of buried nitride layer; (b) base polysilicon deposition; (c) hole defination in base; (d) growth of thin sacrificial oxide; (e) patterning of anchor points; (f) deposition of plug polysilicon; (g) planarization of plug layer; (h) deposition and patterning of protective nitride layer, and through etch; (i) final release of structure in HF [38].

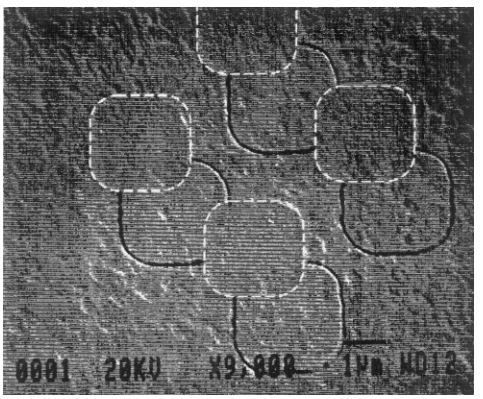

Fig. 9. Micrograph of pores from D1 design with highlighted anchor points [38].

narization of the outer structural layer to expose the total pore area. As with all the membrane protocols, the first step in the fabrication was the etching of the support ridge structure into the bulk silicon substrate. A low stress silicon nitride (LSN or nitride), which functioned as an etch stop layer, was then deposited using low pressure chemical vapor deposition (LPCVD). The base structural polysilicon layer (base layer) was deposited on top of the etch stop layer. Because the etch stop layer did not fill the machined ridges, the structural layer was deposited down into the support ridge, which remained after the membrane was released and the etch stop layer was removed.

The etching of holes in the base layer was what defined the shape of the pores. For this research, the mask consisted of separated square holes (see Fig. 9), but other pore structures could easily be adapted to this protocol. In this step, it was important to make sure the etching went completely through the base layer, so an overetch was used. It is useful to note that the buried nitride etch stop acted as an etch stop for the plasma etching of a silicon base layer. After the pore holes were defined and etched through the base layer, the pore sacrificial oxide was grown on the base layer. The sacrificial oxide thickness determines the pore size in the final membrane, so control of this step was critical to reproducible pore sizes in the membranes. The basic requirement of the sacrificial layer is the ability to control the thickness with high precision across the entire wafer. Thermal oxidation of polysilicon allowed the control of the sacrificial layer thickness of less than 5% across the entire wafer. Limitations on this control came from local inhomogeneities in the polysilicon, such as the initial thickness of the native oxide, the grain size or density, and the impurity concentrations.

Anchor points are defined in the sacrificial oxide layer to mechanically connect the base layer with the plug layer (necessary to maintain the pore spacing between layers). This was accomplished by using the same mask shifted from the pore holes by 1 μm diago-

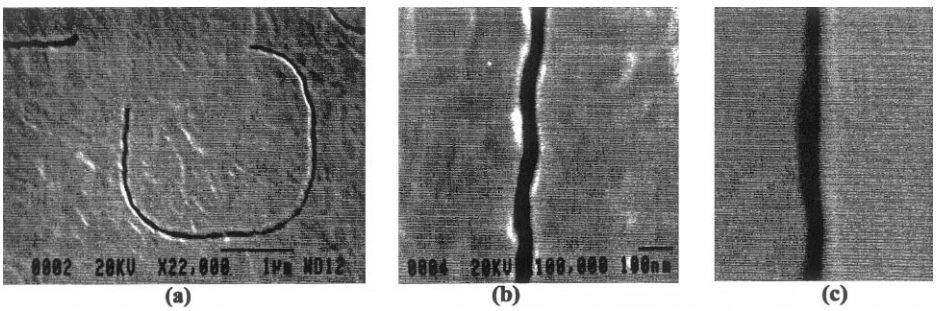


Fig. 10. Pore size measurements showing: (a) single 50 nm pore; (b) high magnification image of 50 nm pore; and (c) high magnification of 25 nm pore [38].

nally (see the defined anchor points in Fig. 9). This produced anchors in one or two corners of each pore hole, which provided the desired connection between the structural layers while opening as much pore area as possible.

After the anchor points were etched through the sacrificial oxide, the plug polysilicon layer was deposited (using LPCVD) to fill in the holes. To open the pores at the surface, the plug layer was planarized using chemical mechanical polishing (CMP) down to the base layer, leaving the final structure with the plug layer only in the pore hole openings.

As the membrane was ready for release, a protective nitride layer was deposited on the wafer (completely covering both sides of the wafer). The backside etch windows were etched in the protective layer, exposing the silicon wafer in the desired areas, and the wafer was placed in a KOH bath to etch. After the silicon wafer was completely removed up to the membrane (as evidenced by the smooth buried etch stop layer), the protective, sacrificial, and etch stop layers were removed by etching in concentrated HF.

Fig. 9 shows a cluster of four pores on a membrane after the release. The square black lines are the pores, showing the location of the plug layer, and the faintly visible squares of solid material, false outlined in a dashed white line, show the location of the anchor points. This pattern is repeated across the entire membrane surface.

To assess the size of the pores fabricated on the D1 protocol membranes, both in situ ellipsometry and post-fabrication microscopy were used. Profiles of the oxide thickness were taken across the wafer, and random measurements around the entire wafer were taken to get a statistical average of the oxide thickness. After the completed fabrication, the pore sizes were measured with a SEM at high magnification and compared to the expected values from the oxide thickness measurements. Fig. 10 shows some of the micrographs obtained for a 25 and a 50 nm pore.

## 3. The micromachined immunoisolation biocapsule

The micromachined immunoisolation biocapsule project started with the general concept of introducing a membrane with highly defined pores into a structure that would allow the microencapsulation of cells for immunoisolation [40]. The biocapsule consists of two separate microfabricated membranes bonded together with the desired cells contained within the cavities. The cavities containing the cells are bounded at the wafer surfaces by microfabricated membrane filters with well-defined pore sizes, to protect the cells from the larger molecules of the body's immune system. A schematic diagram of the microfabricated biocapsule is shown in Fig. 11, showing the exclusion of immune molecules (with sizes of $\geq 15$nm) while allowing the passage of insulin and nutrients (sizes of $\leq 6$ nm).

The basic technology that was developed for the pores themselves was the use of a sacrificial oxide sandwiched between silicon layers, thus defining a space that could be opened by a subsequent etching of the oxide in HF. To make the complete immunoisolation capsule, the silicon substrate is etched up to the membrane, leaving a cavity in the wafer with an encapsulating immunoisolation membrane. Any of the membranes fabrication protocols described in the previous section

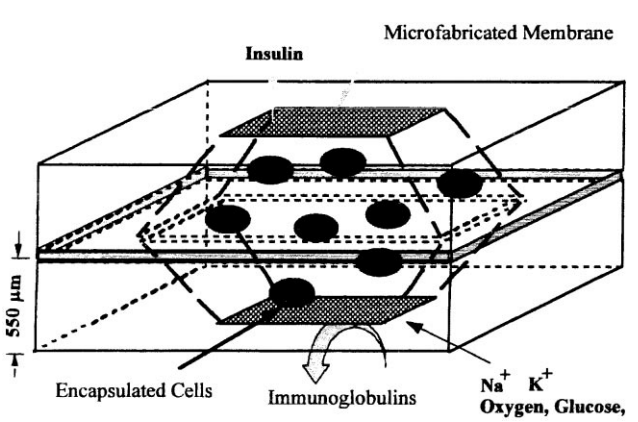


Fig. 11. Diagram of basic microfabricated immunoisolation biocapsule concept.

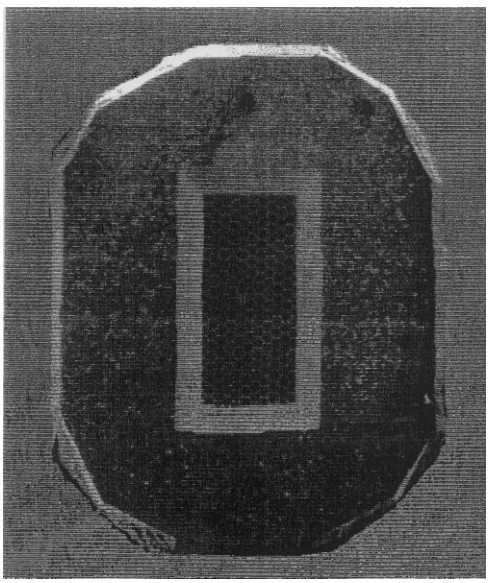

Fig. 12. One-half of immunoisolation biocapsule.

could be used. For the majority of the in vitro and in vivo biocapsule studies, the M2 design was used. This yields a final biocapsule with dimensions of: 1100 μm in thickness, $4 \times 4$ mm in lateral dimensions, membrane area of 10.4 $mm^2$, cavity volume of approximately 10 μl, and a membrane thickness of 9 μm (Figs. 12–14). Isolated islets are suspended in an alginate matrix (2%) to keep cells evenly dispersed. This suspension is gently pipetted into a half-capsule and joined by another half-capsule by an adhesive (medical grade silicone elastomer) to form the full capsule. Prior to use, biocapsules are stored in culture dish wells under appropriate culture conditions (incubation at 37°C, 5% $CO_2$, in 1 ml of RPMI complete medium + 10% fetal bovine serum).

### 3.1. Biocapsule loading and assembly

One major challenges associated with the microfabricated biocapsule is the procedure for bonding the two half capsules together. Due to the close proximity of cells and living tissue to both the internal and external capsule interface, the choice for a suitable bonding agent is nontrivial.

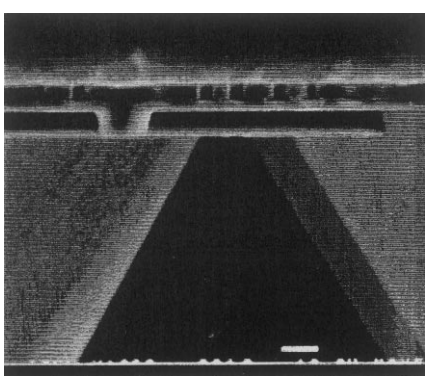

Fig. 13. Cross sectional view of the biocapsule membrane.

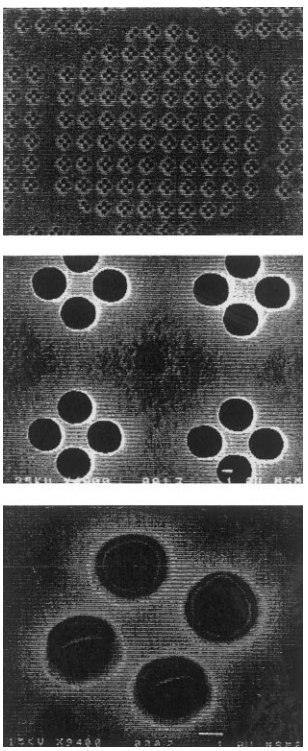

Fig. 14. Top views of micromachined membranes showing entry ports with diffusion channels underneath [43].

Because the cells are placed in the biocapsule before the pieces are bonded together, the bonding process must be able to occur in the presence of the biological materials to be transplanted without affecting their functionality. The microelectronics industry has studied adhesives for standard silicon processing, as needed for the packaging of Ics, but these materials are not acceptable due to their processing temperatures, outgassing problems, or presence of other potentially cytotoxic substances. While research has been performed extensively on adhesives that can be used in biological conditions, especially for dentistry and surgery, there has been little work done on bonding techniques that are specifically non-cytotoxic during the application and curing process on materials such as silicon. The surface chemistry of silicon is quite different from traditional biomaterials and therefore, a biocompatible bonding agent for silicon is not necessarily readily available, nor thoroughly investigated.

In our in vitro studies with fully bonded microfabricated biocapsules, the bonding agent used was a medical grade silicone elastomer (Type A Medical Adhesive, Factor II Inc.). However, we have also developed alternative bonding materials (PPMA, and PEBMA) that have suitable processing temperatures and biologic compatibility. Both PPMA and PEBMA are suitable

bonding agents for the biocapsules. Their non-cytotoxicity is clearly sufficient for use in the presence of live cells ([38]). They both have been used to bond silicon at body temperature (by pressing two pieces of silicon, one coated with the polymer, together between the hands of the investigator), but at that temperature defects become highly relevant. Mechanically, the methacrylates have shown that once properly bonded, they have more than sufficient strength for use in the body. By comparison, PPMA and PEBMA have higher adhesive strengths that PMMA, which is currently used as a bone cement, perhaps one of the most demanding mechanical applications of biomaterials to date. The small size of the devices also greatly limits the stresses that can be experienced, lowering the adhesive requirements well below the strengths of most bonding processes.

Once the membranes were fabricated, the capsule was made by encapsulating cells within a pocket defined by the cavities of two. The pancreatic islets were harvested from neonatal rats using collagenase to digest the extracellular collagen matrix supporting the cells. The cells were concentrated in solution by sedimentation for more densely filled capsules. One half of the capsule was used to hold the cells while the other half had adhesive applied to the bonding areas. By keeping the bonding areas on the cell half clean of biological fluids through careful pipetting, it was possible to form a hermetic, strong seal between the two halves. After the adhesive cures or completes its bonding process, the capsules were backfilled with serum until they were completely filled with fluid and the pores on both membrane sides were wetted with serum [41].

### *3.2. Biocompatibility of nanomembrane and biocapsular environment*

Our preliminary studies centered upon investigating the general biocompatibility of silicon membranes. Direct cell contact tests and long-term bulk material implants indicated a sufficient degree of long-term biocompatibility ([42]). In vivo, the biocompatibility of silicon microimplants was evaluated by implanting square block samples ($3 \times 3 \times 5$ mm$^3$) into the pancreas, liver, spleen and kidney of adult rats. Specimens were fabricated either with 2 mm blind filtration channels cut into the central portions of silicon blocks coated with polysilicon or single crystal silicon blocks with no polysilicon coating. For both groups of silicon microimplants, the surface appearance was the same both before and after the implantation. There appeared to be no changes in the mechanical properties of the implants and no corrosion was observed. The surface of the samples remained smooth although some of the wafers displayed slight tissue adherence. The blind filtration channels appeared clear and free from any obstructions.

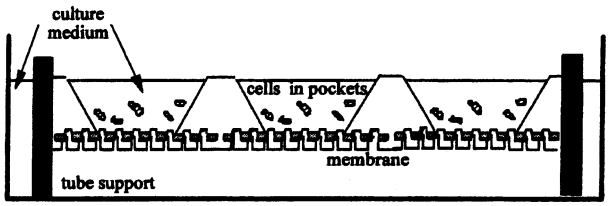


Fig. 15. Cells cultured in arrays of membrane-bounded wells.

The tissue response to the implants was assessed by light microscopy by a modification of the method developed by Salthouse. No significant differences were observed between the two implant types in terms of chronic tissue response. Although a fibrous tissue capsule was maintained by the continuing presence of the implant, the surrounding tissue appeared normal and extremely well vascularized. No gross abnormalities of color or consistency were observed in the tissue surrounding the implant. In general, the fibrous capsule was well-formed and displayed little migration. No necrosis, calcification, tumorgenesis, or infection was observed at any of the implant sites. Overall, our biocompatibility studies suggested that silicon substrates were well-tolerated and non-toxic both in vitro and in vivo, leading to our further studies on islet encapsulation within biocapsules.

The behavior of different cell types in three-dimensional silicon microstructures was studied using microfabricated half-capsules (or culture wafers) (Fig. 15). Cytotoxicity tests were performed by examining the cell morphology, growth, and function of test cell lines placed in contact with arrays of membranes, with promising results. The biocompatibility was evaluated via direct contact tests by cultivating several different cell lines such as macrophages, fibroblasts, and HeLa cells, as well as isolated primary islets of Langerhans both on the wafer surface and within the porous wafer pockets [42] (Fig. 16). All cells were seeded on silicon

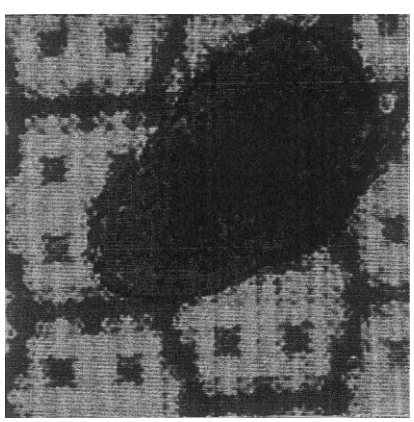

Fig. 16. Pancreatic islet cultured on permselective silicon membrane.

culture wafers, observed via light microscope, stained for cell viability and functionality, and counted with a hemaecytometer. All cell types had normal growth characteristics, morphology, and $>90\%$ viability.

Cell functionality has also been studied in microfabricated silicon three-dimensional permselective environments, with varying pore sizes in the μm- to nm range. Evaluating antibody secretion from hybridomas and insulin secretion from rat islets of Langerhans ([41]) monitored cell functionality. The level of antibody secretion from hybridomas cultured on silicon membranes and in control polystyrene culture wells was similar by western blot analysis, indicating no apparent impairment of hybridoma function in the culture wafer pockets. Overall, islets in microfabricated silicon pockets and the control dishes appeared to have similar morphology and viability. Glucose-supplemented medium was allowed to diffuse to the islets, from underneath the membrane, to stimulate insulin production and monitor cell functionality. Similar levels of insulin secretion were measured for islets within microfabricated cell culture arrays and on control surfaces suggesting that glucose was able to sufficiently pass through the pores of the wafer pockets to stimulate islets for insulin production. The environment of the silicon pockets showed no inhibition of islet functionality and insulin secretion, as compared to control islets [41].

### 3.3. Diffusion studies

Initial diffusion studies were carried with polystyrene beads of various dimensions in a two reservoir diffusion chamber. It was found that biocapsules membranes of 18 nm pore size completely blocked the diffusion of 44 and 100 nm diameter polystyrene beads, while 66 nm pore sized membranes only blocked 100 nm diameter beads. No fluorescent signal above baseline was detected in the incubation medium surrounding 18 nm biocapsules after 1 and 4 days [37].

### 3.4. Glucose and insulin diffusion

The concentration of insulin, secreted by the islets through the membrane, into the surrounding medium was compared between the unencapsulated islets and the islets on micromachined membranes ([43]). The concentration of diffused insulin through the membrane into the medium was compared to the amount of insulin secreted by unencapsulated islets. The amounts were similar in concentration and time release suggesting that glucose was able to sufficiently pass through the pores of the wafer pockets to stimulate islets for insulin production.

Results indicated that the insulin secretion by the islets and subsequent diffusion through the biocapsule membrane channels was similar to that of unencapsulated islets for both 3 μm and 78 nm pore sized membranes, with insulin diffusion though the membrane occurring within ten minutes of stimulation. Fig. 17 shows the typical insulin release profile in response to stimulatory (16.7 mM) glucose medium over 1 hour under static incubation for 78, 66, and 18 nm pore-sized membranes. This profile indicated that insulin and glucose diffusion occurred at sufficiently high rates through the microfabricated membrane to ensure nutrient exchange for encapsulated islet cells. These experiments show that no diffusion barrier is formed by the membrane for glucose and insulin, while taking into account the effect of rotation on mass transfer.

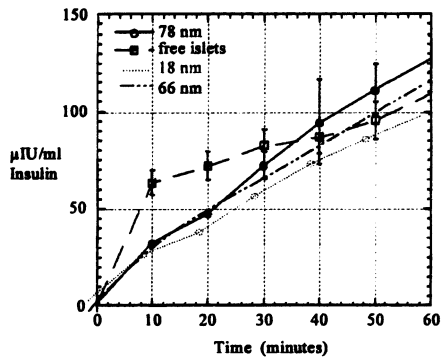


Fig. 17. Insulin secretory profile through differing pore sizes.

### 3.5. IgG diffusion

The data indicated that microfabricated biocapsule membranes could be tailormade to attain desired IgG diffusion kinetics. At the same time, the complete deselection of IgG requires absolute pore dimensions below 18 nm. This refines the previous understanding that pore in the range 30–50 nm would suffice to provide membrane-based immunoisolation [7]. With reference to the data reported in Fig. 18, it is noted that the percent of IgG diffusion (concentration of IgG that passes through the membrane) was less than 0.4% after 24 h and 2% after over 150 h through the 18 nm membranes. Compared to commonly used polymeric membranes, this rate was several times smaller indicating superior immunoprotection. For example, Dionne et al. measured an IgG concentration of 1% after 24 hours through poly(acrylonitrile-co-vinyl chloride) membranes with a molecular weight cut-off of $\approx 80\,000$ MW ([44]). Although the IgG molecule has a molecular weight of approximately 150 kD, studies have disagreed on the actual dimensions of the molecule, estimated to be tens of nm or less. For example, Wang and colleagues (1997) investigated permeability of relevant immune molecules to sodium alginate/poly-L-lysine capsules and found that significant amounts of IgG (close to 40%) passed through both 230 and 110 kD membranes in 24 h [12].

### 3.6. Islet immunoprotection

As shown in Fig. 19, the 18 nm biocapsules seem to provide significant immunoprotection to those islets encapsulated within its semi-permeable membrane. After 2 weeks in culture with antibodies and serum complement, islets in microfabricated biocapsules maintained close to original glucose stimulated insulin secretory capability even after 2 weeks in the presence of antibodies and complement. Islets immunoprotected by 18 nm pore-sized membrane maintained their functionality better than those in 78 nm pore sized biocapsules, confirming that greater immunoprotectiveness was offered by 18 nm membranes. In contrast, there was a marked decrease in baseline and stimulated response in free islets.

### 3.7. Studies on the short-term immunoisolation of insulinoma xenografts

Microfabricated biocapsules incubated in vitro for 8 days showed stimulus secretion coupling of glucose and insulin for encapsulated insulinoma cells (Table 1). As shown in Fig. 20, the static incubation study resulted in insulin secretion from the microfabricated biocapsules containing RIN cells in response to basal glucose levels and stimulatory glucose (2.8 mmol/l) levels. The stimulatory index (SI = stimulatory/basal insulin secretion) in picograms (pg) for RIN cells in 18 nm pore-sized microfabricated biocapsules was approximately 1.9. In 66 nm pore-sized biocapsules, the basal value was $12.0 \pm 5.65$ and jumped significantly to $71.3 \pm 17.25$ under stimulatory conditions, a 5.9-fold increase. Similarly, encapsulated βTC6F7 cells also displayed basal and stimulatory (16.7 mmol/l) insulin release, with a SI of 4.3 for 18 nm pore-sized biocapsules. Biocapsules of 66 nm pore-size containing βTC6F7 cells had a SI value of 9.2 in vitro [45].

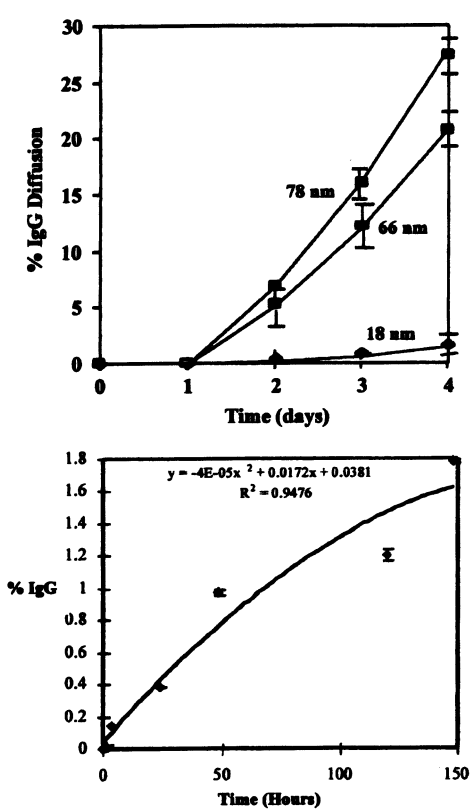


Fig. 18. IgG diffusion through microfabricated biocapsules of (a) three different pore sizes and (b) 18 nm pore-sized membrane [43].

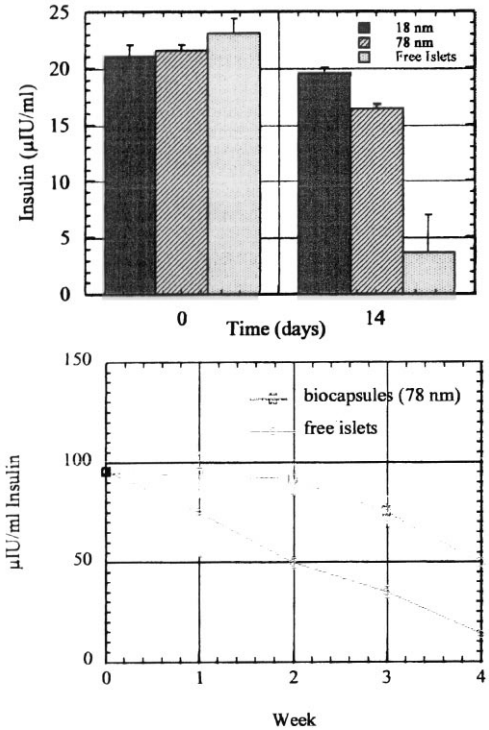


Fig. 19. Insulin secretion of islets within different pore-sized biocapsules and unencapsulated incubated for (a) 2 weeks with seerum complement/antibody solution (20 islets/biocapsule, $n = 6$) and (b) over 1 month [41].

### 3.8. In vivo study

Microfabricated biocapsules filled with either RIN or βTC6F7 cells were also implanted into mice. After 8

Table 1
Insulin secretion from glucose stimulated biocapsules where SI = stimulatory index (stimulatory insulin secretion over basal insulin secretion)

| Cell | | SI (18 nm) | SI (66 nm) |
|---|---|---|---|
| RIN | In vitro | $1.5 \pm 0.4$ | $1.7 \pm 0.2$ |
| | In vitro | $1.9 \pm 0.05$ | $5.9 \pm 0.9$ |
| βTC6F7 | In vitro | $3.6 \pm 0.3$ | $1.7 \pm 0.2$ |
| | In vitro | $4.3 \pm 0.7$ | $9.2 \pm 0.5$ |

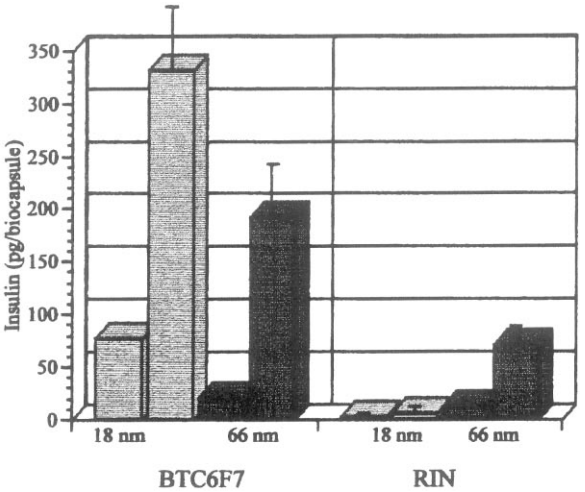


Fig. 20. In vitro insulin secretion from RIN and βTC6F7 filled biocapsules in response to basal and stimulatory glucose levels. Mean values are expressed in pg insulin released ( ± SD) per 18 or 66 nm pore sized biocapsule [46].

days of intraperitoneal implantation, glucose stimulated insulin secretion from the retrieved biocapsules was examined under static conditions ([46]). Microfabricated biocapsules were easily located in the abdominal cavity of laparotomized mice. Three biocapsules remained in the original implantation site, while the remaining biocapsules migrated to either the abdominal cavity, bowel loops, or mesentery. Nonetheless, all biocapsules seemed mechanically intact with no macroscopic changes in surface architecture or properties. Tissue surrounding the biocapsules found in their original implantation site showed no abnormalities while tissue around two of the migrated biocapsules displayed minor neutrophil infiltration. This could reflect poor surgical implantation or sterile techniques. Some capsules ($n = 4$) had agglutinated during their migration but were mechanically intact nonetheless.

In vivo, the βTC6F7 cells remained viable in microfabricated environments. The stimulatory index for 18 nm and 66 nm pore size microfabricated biocapsules was 3.6 and 1.75, respectively. The xenogeneic RIN cells encapsulated in 18 nm biocapsules were also able to maintain their functionality and displayed basal and stimulatory insulin secretion of $2.23 \pm 0.12$ and $3.10 \pm 0.5$, corresponding to a stimulatory index of approximately 1.5. In 66 nm pore sized biocapsules, RIN cells had a stimulatory index of approximately 1.7. In contrast, the freely injected RIN and βTC6F7 cells were undetectable in the peritoneum as well as in any other organ (liver, kidney, lungs, or brain) as determined by careful autopsy. The peritoneum is known to elicit a strong immune reaction to these free insulinoma cells. Viable free insulinoma cells are expected to form a tumor nodule. However, it was nonetheless observed that all $2 \times 10^5$ free insulinoma cells were completely taken up by the immune system while encapsulated insulinoma cells survived and maintained functionality (Fig. 21).

Several issues regarding microfabricated biocapsule implantation and effectiveness were revealed in these experiments. Insulinoma cells did maintain their viability within microfabricated biocapsules over the studied period. However, it was shown that encapsulated βTC6F7 cells in vitro maintained a greater stimulatory insulin response than in vivo. Also, the size of the pores of the biocapsule greatly affected the secretory response. The lower insulin response in the 66 nm biocapsules implanted compared to the implanted 18 nm biocapsules could be attributable to the penetration of immune molecules through the relatively larger membrane pores and subsequent attack of encapsulated insulinoma cells. The effective size of antibody and complement components of the immune system has been hypothesized to be between 20 and 50 nm. Previous studies on biocapsules have suggested that pore sizes smaller than 100 nm are effective in hindering passage but still do not completely block immune molecules from reaching the target cell [23]. Therefore, it is likely that a pore size of 66 nm still allows passage of immune molecules. Comparing the stimulatory indices of βTC6F7 cells in 18 and 66 nm pore-sized capsules in vitro, we find that the indices are approximately 4 and 9, respectively (Table 1). This suggests that the larger pores of the 66 nm capsules are more effective in facilitating nutrient diffusion to the encapsulated cells, leading to greater cell viability. This behavior is echoed in the case of RIN cells *in vitro*, where indices are approximately 2 and 6 for 18 and 66 nm biocapsules, respectively.

Turning to the explanted biocapsules, we observed stimulatory indices of approximately 4 and 2 for

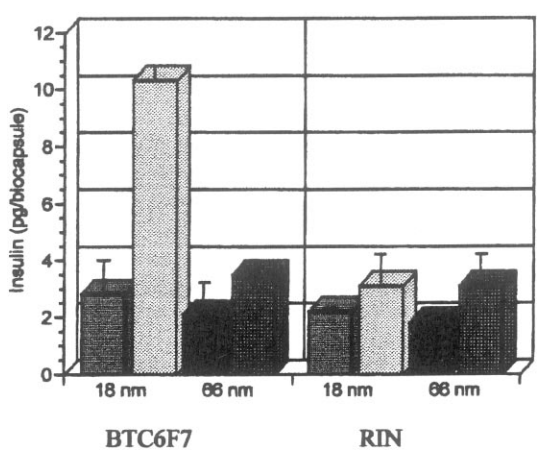


Fig. 21. Insulin secretion from RIN and βTC6F7 filled biocapsules in response to basal and stimulatory glucose levels after 1 week intraperitoneal implantation. Mean values are expressed in pg insulin released ( ± SD) per 18 or 66 nm pore sized biocapsule [46].

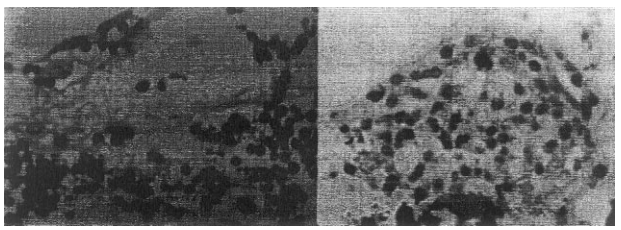

Fig. 22. Unencapsulated islet with lymphoctic infiltration (left) and immunoprotectd islet encapsulated within micromachimed biocapsule (right) after 2 week implantation.

βTC6F7 cells in 18 and 66 nm pore-sized capsules, respectively (Table 1). Similarly, RIN cells in explanted 18 and 66 nm pore-sized capsules both had indices of approximately 2. We observed that a sharp reduction in the stimulatory indices of both cells lines in 66 nm biocapsules, whereas the stimulatory indices of explanted 18 nm capsules remains essentially the same as that which was observed for *in vitro* 18 nm biocapsules. This seems to indicate the immunoisolatory effect of 18 nm pore-sized biocapsules and the lack of effective immunoisolation by the 66 nm biocapsules. These results were supported with short term studies on human pancreatic islets transplanted into rats. As Fig. 22 illustrates, human islets encapsulated in capsules and implanted in rats also revealed short term immunoisolation [41].

## 4. Conclusions

Research over the past few years has shown that the micromachined membrane structures can be used as carrier biocapsules for the implantation of cells for the treatment of Type I diabetes as well as for biomolecular separation applications. An 18 nm pore membrane showed high enough glucose and insulin diffusion rates to allow proper passage of the molecules to encapsulated pancreatic islets while preventing the passage of the majority of immune molecules such as IgG. Further optimization of the pore size configuration is necessary for absolute retention of immune molecules, but the control of the pore geometry fabrication facilitates this optimization. The precise control of the pore channel geometries afforded by the microfabrication protocol will allow us to determine the exact pore size that prevents the passage of immune molecular, and therefore will allow us to protect transplanted cells adequately and analyze individual biomolecules through separation methods.

## Acknowledgements

Parts of this work were supported by NSF (ECS #9820829) (TAD), the Whitaker Foundation (TAD), and Microfab BioSystems (MF). Special thanks to the Berkeley Microfabrication Laboratory where much of this work was performed.

## References

[1] Aebischer P, Winn SR, Galletti PM. Brain Res 1988;448:364–8.
[2] Colton CK. Cell Transplant 1995;4:415–36.
[3] Fu XW, Sun AM. Transplantation 1989;47:432–5.
[4] Lim F, Sun AM. Science 1980;210:908–10.
[5] Colton CK, Avgoustiniatos ES. Trans ASME 1991;113:152–70.
[6] Scharp DW, Mason NS, Sparks RE. World J Surg 1984;8:221–9.
[7] Lanza RP, Sullivan SJ, Chick WL. Diabetes 1992;41(2):1503–10.
[8] O'Shea GM, Goosen MFA, Sun AM. Biochim Biophys Acta 1984;804:133–6.
[9] Chaikof EL. Ann Rev Biomed Eng 1999;1:103–27.
[10] Robitaille R, Paiseau J-F, Leblond FA, Lamourex M, Lepage Y, Hallé J-P. J Biomed Mater Res 1999;44:116–20.
[11] Siebers U, Horcher A, Bretzel RG, Federlin K, Zekorn T. Alginate-based microcapsules for immunoprotected islet transplantation. Ann NY Acad Sci 1997;31(831):304–12.
[12] Wang T, Lacik I, Brissova M, Anilkumar AV, Prokop A, Hunkeler D, Green R, Shahrokhi K, Powers AC. Nature Biotechnol 1997;15:358–62.
[13] Dixit V, Gitnick G. J Biomater Sci Polymer Ed 1995;7:343–57.
[14] Wells GDM, Fisher MM, Sefton MV. Biomaterials 1993;14:615–20.
[15] Tresco PA, Winn SR, Aebischer P. Am Soc Art Int Organs J 1992;38:17–23.
[16] Lum Z-P, Krestow M, Tai IT, Vacek I, Sun AM. Transplantation 1992;53:1180–3.
[17] Lafferty KJ. Diabetes Nut Metab 1989;2:323–32.
[18] Goosen M. Biotechnol Bioeng 1985;27:146–50.
[19] van Schilfgaarde R, de Vos P. Factors influencing the properties and performance of microcapsules for immunoprotection of pancreatic islets. J Mol Med 1999;77(1):199–205.
[20] Lacy P. Science 1992;254:1728–34.
[21] Altman JJ. In: Ricordi C, editor. Pancreatic Islet Cell Transplantation, 1991:216–22.
[22] Ross, P.E. (1993). Living Care. Scientific American, pp 18–20, June 1993.
[23] Iwata H., Morikawa N., Fujii T., Takagi T., Samejima, Ikada Y. Does immunoisolation need to prevent the passage of antibodies and complement? Transplant. Proc. 1995;27(6):3224–3226.
[24] Lanza, R.P., Chick, W.L. Encapsulated cell therapy. Sci. Am. Sci. Med. 1995;2:16–25.
[25] Chang TM. Artificial cells, encapsulation, and immobilization. Ann NY Acad Sci 1999;18(875):71–83.
[26] Baxter GT, Bousse LJ, Dawes TD, Libby JM, Modlin DN, Owick JC, Parce JW. Microfabrication in silicon microphysiometry. Clin Chem 1994;40(9):1800–4.
[27] Wooley AT, Mathies RA. Ultra high-speed DNA fragment separations using microfabricated capillary array electrophoresis chips. Proc Natl Acad Sci USA 1994;91:11348–52.
[28] Gourley PL. Semiconductor microlasers: a new approach to cell-structure analysis. Nat Med 1996;2(8):942–4.
[29] Edell DJ, Churchill JN, Gourley IM. Biocompatibility of a silicon based peripheral nerve electrode. Biomat Med Dev Artif Org 1982;10(2):103–22.
[30] Kovacs GTA, Storment CW, Halks-Miller M, Belczynski CR, Della Santina CC, Lewis EA, and Maluf NI. Silicon-substrate microelectrode arrays for parallel recording of neural

activity in peripheral nerves. IEEE Transact. Biomed. Eng. 1994;41:567–77.
[31] Wise KD, et al. Micromachined silicon microprobes for CNS recording and stimulation. Ann Conf IEEE Eng Med Biol Soc 1990;12(5):2334–5.
[32] Chu W-H, Ferrari M. SPIE Microfabrication SPIE, vol. 2593. CA: San Jose, 1995.
[33] Yang X, Yang JM, Wang XQ, Meng E, Tai YC, Ho CM. Micromachined Membrane Particle Filters 1998.
[34] Rijn CJMV, Veldhuis GJ, Kuiper S. Nanotechnology 1998;9:343–5.
[35] Kittilsland G, Stemme G, Norden B. Sensors Actuat 1990;A21-A23:904–7.
[36] Chu, W.-H., Ferrari, M. 1998 US Patents # 5 798 076 and # 5 798 042 Regents of the University of California, USA.
[37] Chu W-H, Chin R, Huen T, Ferrari M. J MicroElectroMech Sys 1999;8:34–42.
[38] Hansford DJ. Materials Science and Mineral Engineering. Berkeley, CA: University of California, 1999.
[39] Hansford, D., Ferrari, M. (to be published).
[40] Ferrari, M., Chu, W.-H., Desai, T., Hansford, D., Mazzoni, G., Huen, T., Zhang, M. (1996). In: Cottrell, C. (Ed.), Thin Films and Surfaces for Bioactivity and Biomedical Application Volume number 414. Boston, MA, pp. 101–106.
[41] Desai TA, Chu WH, Tu JK, Beattie GM, Hayek A, Ferrari M. Biotechnol Bioeng 1998;57:118–20.
[42] Desai TA, Ferrari M, Mazzoni G. Silicon microimplants: fabrication and biocompatibility. In: Kozik T, editor. Materials and Design Technology. ASME, 1995:97–103.
[43] Desai TA, Hansford D, Kulinsky L, Nashat A, Rasi G, Tu J, Wang Y, Zhang M, Ferrari M. Nanopore technology for biomedical applications. J Biomed Microdev 1999;2(1):11–40.
[44] Dionne KE, Cain BM, Li RH, Bell WJ, Doherty EJ, Rein DH, Lysaght MJ, Gentile FT. Biomaterials 1996;17:257–66.
[45] Desai T.A., Hansford D.M., Ferrari. Characterization of Micromachined Membranes for Immunoisolation and Bioseparation Applications. J. Membrane Sci., 1999;4132:1–11.
[46] Desai TA, Chu WH, Rasi G, Vallebona PS, Guarino E, Ferrari M. Microfabricated biocapsules provide short-term immunoisolation of insulinoma xenografts. J Biomed Microdev 1999c;1(2):131–81.